UDK 621.316.13

INVESTIGATION OF ELECTROMAGNETIC PROCESSES IN THE CASE OF STATIC ECCENTRICITY OF A TWO-POLE INDUCTION MOTOR WITH A SHORT-CIRCUITED ROTOR

KOTSUR I.M. PhD, Associate Professor of the Electrical Machines Department, National University "Zaporizhzhia Polytechnic", Zaporizhzhia, Ukraine, e-mail: igor.m.kotsur@gmail.com , ORCID: https://orcid.org/0000-0001-6394-7849 ;

KOTSUR M.I. PhD, Associate Professor of the Electrical and Electronic Devices Department, National University "Zaporizhzhia Polytechnic", Zaporizhzhia, Ukraine, e-mail: kotsur_m@ukr.net, ORCID: https://orcid.org/0000-0002-0072-5437;

YARYMBASH D.S. Dr. Sc. (Tech.), Professor, Head of the Department of the Electrical Machines Department, National University "Zaporizhzhia Polytechnic", Zaporizhzhia, Ukraine, e-mail: yarymbash@gmail.com, ORCID: https://orcid.org/0000-0003-2324-9303;

DYVCHUK T.Ye. PhD, Associate Professor of the Electrical Machines Department, National University "Zaporizhzhia Polytechnic", Zaporizhzhia, Ukraine, e-mail: tetiana.divchuk@gmail.com, ORCID: https://orcid.org/0000-0002-8779-2615;

BEZVERKHNIA Yu. S. PhD, Associate Professor of the Electrical Machines Department, National University "Zaporizhzhia Polytechnic", Zaporizhzhia, Ukraine, e-mail: juliakafedraem@gmail.com , ORCID: https://orcid.org/0000-0002-8779-2615;

OZEROV V.S. Master of the Department of Electric Machines at Zaporizhzhia National University 'Zaporizhzhia Polytechnic', Zaporizhzhia, Ukraine, e-mail: vovavorobiov@gmail.com, ORCID: https://orcid.org/0009-0009-8059-7911

Purpose. *Correction of the mathematical model of electromagnetic processes in a two-pole induction motor with a short-circuited rotor, taking into account static rotor eccentricity to identify diagnostic correlations.*

Methodology. *Analytical modeling using the method of specific magnetic conductivity, mathematical modeling of electromagnetic fields in a three-phase induction motor with a short-circuited rotor using methods of electromagnetic field theory and finite element methods.*

Obtained results. *The necessity of improving mathematical models for induction motors with short-circuited rotors to establish new or refine connections between diagnostic features and diagnosed defects has been demonstrated. Refined mathematical expressions for calculating the specific conductivity of non-uniform air gaps in induction motors with static eccentricity are provided. Modeling was performed using the FEMM environment for a statically eccentric two-pole induction motor with a short-circuited rotor. It has been proven that the harmonic order values obtained using the numerical-field method are consistent with those obtained analytically.*

Findings. *Based on the field approach and using the finite elements method, an analysis of the distribution of magnetic field in a two-pole induction motor with a short-circuited rotor was conducted. Harmonic analysis of the magnetic field in the air gap was performed to identify the fundamental harmonic and higher and lower-order harmonics when eccentricity occurs. The influence of static rotor eccentricity on the electromagnetic processes of the induction motor was analyzed.*

Practical value. *The results of the study can be utilized for functional diagnosis of the rotor winding of induction motors based on the radial component of the magnetic field. This will contribute to enhancing the reliability of induction motors and enable the prevention of failure in induction motors with short-circuited rotors.*

Keywords: induction motor, static eccentricity, mathematical model, Fourier series, error, magnetic conductivity, amplitude, harmonic.

I. INTRODUTION

Induction motors (IM) with short-circuited rotors are widely utilized across various industries for electricity generation and as electric drives. Recently, there has been increasing attention to the diagnosis of induction motors (IM) aimed at preventing sudden failures and improving the technical and economic performance of their utilization. In induction motors (IM), rotor eccentricity often occurs, which is accompanied by non-uniformity in the

DOI 10.15588/1607-6761-2023-4-2

air gap. [1]. According to various sources [1], from 20 to 40% of failures in induction motors are attributed to eccentricity, which can be caused by manufacturing technological errors, wear during usage, violation of operating conditions, and due to poor repair quality.

In general, there are two types of eccentricity: static eccentricity (which remains unchanged in time and space) - the eccentric position of the rotor in the stator slot; and dynamic eccentricity - the misalignment of the rotor surface with respect to its axis of rotation.

The practice of operating induction motors shows that a significant portion (up to 50%) [4] – [7] operates for extended periods with static eccentricity (SE) of the rotor, which significantly exceeds their technological eccentricity (tolerated during manufacturing). The static eccentricity (SE) of the rotor in induction motors can be caused by inaccuracies in the manufacturing of bearing shields and stators, incorrect centering of the rotor, and misalignment of the drive mechanism. Static eccentricity (SE) in induction motors can also occur during operation. In this case, its appearance may be caused by bearing wear or damage, displacement of supports, or external forces acting on the rotor shaft.

The operation of induction motors with rotor static eccentricity (SE) within the air gap does not immediately lead to its failure, but it does result in deterioration of electromechanical characteristics, energy performance, and consequently, an increase in additional energy losses. Rotor eccentricity in induction motors is accompanied by non-uniformity in the air gap, which, in turn, leads to the emergence of additional magnetic fields.

Distortion of the magnetic field in the air gap creates unidirectional magnetic pull [9], resulting in a decrease of maximum and starting torques within 20% and 8% respectively, while slip increases by 10% [11]. Local heating and motor vibration increase, and additional harmonic components appear. As a result, the reliability and service life of the induction motor decrease. With significant displacement, the rotor begins to come into contact with the stator (see Figure 1), leading to significant heating of their cores, melting or damage to the "squirrel cage". This accelerates the deterioration of the stator winding insulation with subsequent short-circuiting within it. Typically, the cost of a major repair of the motor after such damage is comparable to the cost of the motor itself.

In the study [4], the authors noted that general-purpose two-pole induction motors with medium power ratings up to 1000 V, after the first rewinding of the windings, subsequently experience a much higher frequency and intensity of sudden failures, mainly associated with static eccentricity (SE) [4].

Figure 1. Contact of the rotor with the stator of the induction motor due to the presence of static eccentricity

Timely detection of the presence and magnitude of rotor eccentricity will not only reduce electricity consumption but also prevent damage to the IM motor.

II. ANALYSIS OF LAST RESEARCHES

There are several main methods of diagnosing electric motors: vibration analysis, electromagnetic (based on measuring electromagnetic fields), and thermal methods.

Electromagnetic diagnostics are based on measuring electromagnetic fields and are quite relevant as they provide accurate diagnostics without direct access to the induction motor. They are based on the principle that any disturbances during the operation of the electrical or mechanical components of the AC motor directly lead to changes in the magnetic fields in the air gap. In the work [11], a methodology for diagnosing the wear of sleeve bearings in AC motors is proposed based on changes in the amplitude values of electromagnetic induction in the air gap of the motor. In this case, the diagnosis of the bearing condition is carried out during the operation of the electric motor.

The magnetic field in the air gap of the electric motor can be accurately modeled using the method of specific magnetic conductivity [1].

For mathematical modeling of the air gap at various values of eccentricity, it is necessary to consider the dependence of the specific magnetic conductivity of the gap on the rotor angle rotation.

Traditionally, to calculate the specific magnetic conductivity of a smooth air gap with rotor eccentricity mathematical expressions obtained by expanding into a Fourier series are used [4]. In article [5], a specific case is considered where eccentricity occurs when one of the rotor supports is removed. Therefore, a modeling approach is proposed by expanding into a Fourier series the dependence of the average value (for all laminations of the rotor core) of the specific magnetic conductivity of the air gap on the angle along the air gap, taking into account the serration of the air gap.

Other variants of eccentricity, such as radial displacement of the rotor axis relative to the longitudinal axis of the stator, are not considered. In all cases, only the zeroth and first terms of the series are considered.

Despite the thorough examination of specific aspects of modeling the magnetic permeance in the air gap under rotor eccentricity, the complete picture of determining the specific magnetic conductivity of this gap is not fully revealed, especially at high values of eccentricity.

There is a sufficient number of modern computer programs that implement the solution of electromagnetic field differential equations using the finite element method, such as ANSYS, Maxwell, FEMM, and others. In this work, calculations of magnetic presence are carried out using the FEMM program, which has several advantages, such as simplicity, low system requirements, and an open license.

A significant number of scientific works [2] – [7] are dedicated to the study of electromagnetic processes in squirrel-cage rotor induction motors with eccentricity. A distinctive feature of publications [6] – [12] is the application of field methods for analyzing electromagnetic processes in induction motors, with the determination of influencing factors. This ensures the identification and justification of reliable diagnostic signs of rotor eccentricity.

For the improvement of electromagnetic diagnostics, detailed research and analysis of electromagnetic processes in squirrel-cage rotor induction motors with static eccentricity are necessary. This requires numerical-field determination of electromagnetic and energy parameters.

III. FORMULATION OF THE WORK PURPOSE

The aim of the study is to improve the mathematical model of electromagnetic processes in a two-pole squirrel-cage induction motor with a short-circuited rotor, considering static rotor eccentricity, in order to establish new or refine existing relationships between diagnostic indicators and diagnosed defects.

IV. EXPOUNDING THE MAIN MATERIAL AND RESULTS ANALYSIS

Static eccentricity occurs when the rotor axis is displaced radially or angularly relative to the longitudinal axis of the stator, while the stator and rotor axes remain mutually immobile [13].

The magnitude of the relative static eccentricity is typically accepted as:

$$\varepsilon = \frac{d}{\delta_m} \tag{1}$$

where d - the displacement of the rotor axis from the stator axis; δ_m – the magnitude of the nominal air gap between the rotor and stator in concentric position

In static eccentricity, the air gap magnitude is solely a function of the rotor position (angle of rotor rotation). The configuration of the air gap and its minimum value remain unchanged over time [14]:

$$\delta(\alpha) = \delta_m \cdot (1 - \varepsilon \cdot cos(\alpha))$$

The variation of the air gap magnitude under static eccentricity is depicted in Figure 3.

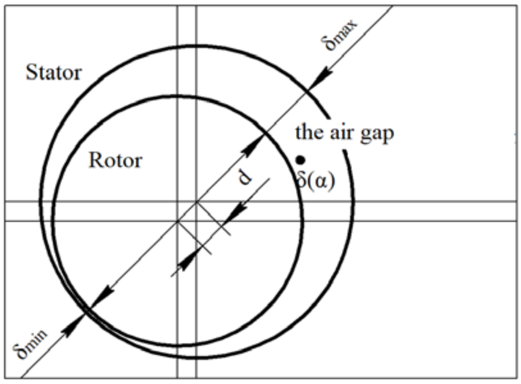

Figure 2. Schematic diagram of the motor under static eccentricity

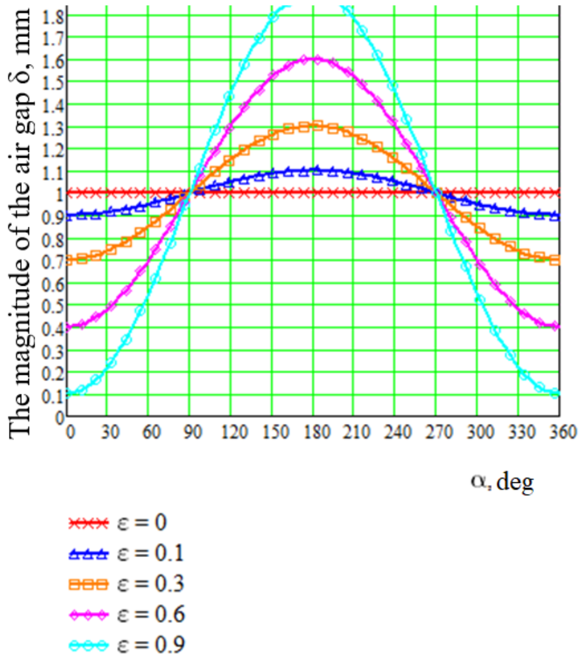

Figure 3. Dependency $\delta(\alpha)$ at $\delta_m = 1mm$

From Figure 2, it follows that under static eccentricity, in the regions of (0, 90) and (270, 360) degrees, the magnitude of the air gap is less than that in a motor operating normally, leading to a decrease in specific magnetic conductivity (Figure 4).

According to the specific magnetic conductivity method, the magnetic field in the air gap is determined by the expression [8], [14] - [17]:

$$B_\delta(\alpha) = F(\alpha,t) \cdot \Lambda_\delta(\alpha,t) \tag{2}$$

where $F(\alpha,t)$ – the magneto motive force in the air gap (generally equal to the sum of the reluctances of the stator winding and the rotor cage), A; α – angular coordinate from the inner circle of the stator ; Λ_δ – specific magnetic conductivity of the air gap, H/m^2 .

In the presence of eccentricity in the air gap, additional conductivity harmonics arise, which are determined by expanding the conductivity of the non-uniform gap into a Fourier series [7], [18]:

$$\Lambda(\alpha)=\frac{\mu_0}{\delta_m}\cdot\sum_{k=0}^{\infty}\lambda_k\cdot cos(k\cdot\alpha) \quad (3)$$

where λ_k – the amplitude of the k-th harmonic of conductivity of the air gap.

The dependency of the specific magnetic conductivity of the smooth air gap on the angle during rotor eccentricity according to [4] is given by:

$$\Lambda=\frac{\mu 0}{\delta_m}\cdot\frac{1}{1-\varepsilon\cdot\cos(\alpha)} \quad (4)$$

Expanding the second multiplier of this expression into a Fourier series, have:

$$\Lambda(\alpha)=\frac{\mu_0}{\delta_m}\cdot\left(\lambda_0+\sum_{k=1}^{\infty}\lambda_k\cdot cos(k\cdot\alpha)\right) \quad (5)$$

where the general term of the series is

$$\lambda_k=2\cdot\frac{\left(1-\sqrt{1-\varepsilon^2}\right)^k}{\varepsilon^k\cdot\sqrt{1-\varepsilon^2}} \quad (6)$$

By the d'Alembert criterion, the series converges when $\varepsilon \prec 1$ [19].

The results of modeling the specific magnetic conductivity of the air gap in the form of a Fourier series are graphically represented in Figure 3 and Figure 4.

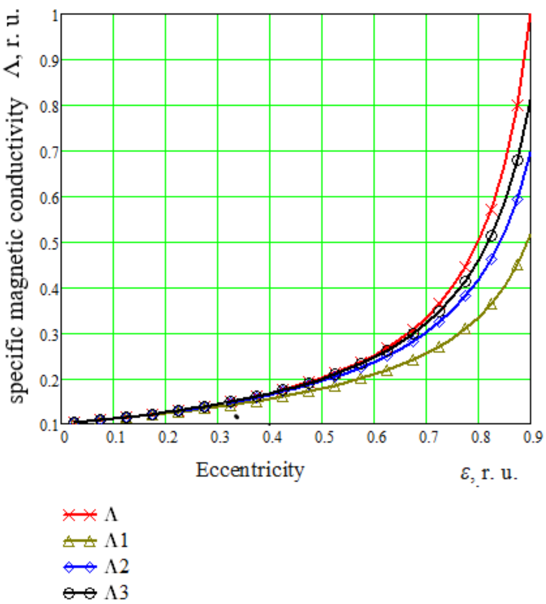

Figure 4. Dependence of the specific magnetic conductivity of the air gap on the eccentricity for different numbers of terms in the series

The dependence of the specific magnetic conductivity of the air gap $\Lambda(\varepsilon)$ on the eccentricity exhibits a strongly pronounced non-linear character. If only the first two terms of the series are considered, starting from a value of ε =0.5 If only the first two terms of the series are considered, starting from a value of $\Lambda(\varepsilon)$ sharply decreases. For example, at ε =0.9 the error in determination will reach 40%. Accounting for the third and fourth terms of the series reduces it by more than 10 times (to 8%).

In Figure 4, the results of modeling the distribution of the specific magnetic conductivity of the air gap as a function of the geometric angle α in the polar coordinate system for different numbers of series terms are presented.

The spatial distribution of the magnetic field induction in the air gap at ρ=1 according to [4] and considering the expansion of the specific conductivity of the non-uniform gap into a Fourier series:

$$B(\alpha)=\frac{\mu_0}{\delta_m}\cdot\lambda_0\cdot F_{ml}\cdot\left(cos(\alpha)-\frac{\lambda_1}{2\cdot\lambda_0}+\right.$$

$$\left.+\sum_{k=1}^{\infty}\left(\frac{\lambda_k}{2\cdot\lambda_0}\cdot cos(\alpha\cdot(k\pm 1))-\frac{\lambda_k\cdot\lambda_1}{2\lambda_0^2}\cdot cos(k\alpha)\right)\right) \quad (7)$$

Based on this expression, harmonics of order p±1 arise in the air gap due to the eccentricity, which rotate induct only with the rotor, caused by the components of the magnetic conductivity. When considering all the terms of the expansion $\Lambda(\alpha)$ expanding into a Fourier series, we obtain that in the air gap of the machine, harmonics with the number of pole pairs p±k (where k = 1, 2, 3…) and the order $v=1\pm k/p$ are present, caused by periodic changes in magnetic conductivity.

In Figure 5, the results of modeling the distribution of the magnetic field induction in the air gap at ρ=1 as a function of the geometric angle α are presented in the polar coordinate system for different numbers of series terms.

To calculate the magnetic field using the finite element method in the FEMM program, a model of the active part of the IM in its cross-section has been created. The physical-geometric model of the active part of the IM is presented in Figure 4. The algorithm for its formation and justification is described in detail in [3].

Numerical calculations of the magnetic field and determination of the necessary electromagnetic parameters were automated using a specially created script in the Lua programming language, integrated into the FEMM program, and presented in the polar coordinate system.

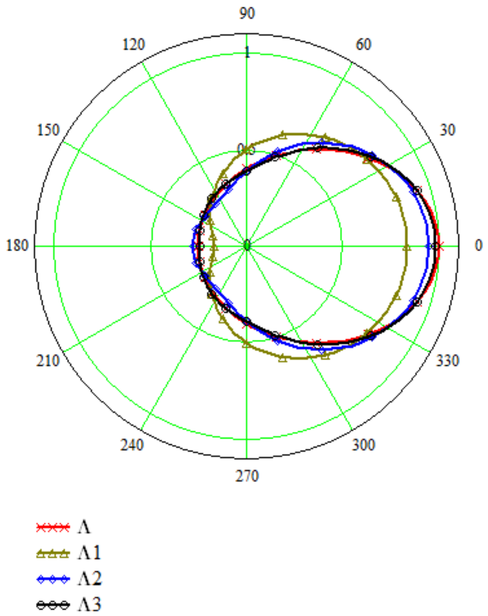

Figure 5. The dependence of the specific magnetic conductivity of the air gap on the geometric angle for different numbers of series terms

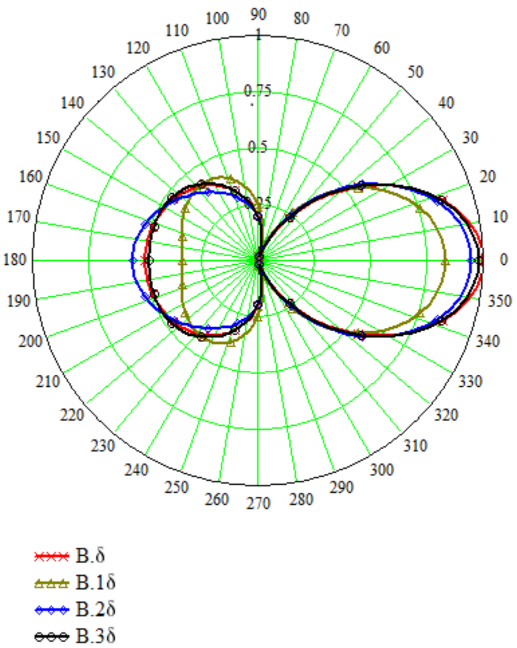

Figure 6. Distribution of magnetic field induction in the air gap at ρ=1 as a function of the geometric angle α in the polar coordinate system for various numbers of series terms

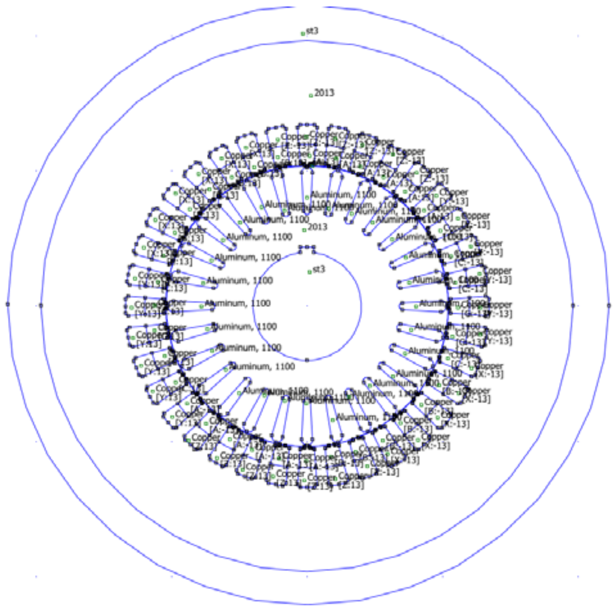

Figure 7. Physical-geometric model of the active part of the AC machine

The differential equation of the stationary magnetic field in the transverse cross-section in the polar coordinate system looks like this [6], [9], [19]:

$$\frac{1}{r}\cdot\frac{\partial}{\partial r}\cdot\left[\nu\cdot r\cdot\frac{\partial A_z}{\partial r}\right]+\frac{1}{r^2}\cdot\frac{\partial}{\partial\varphi}\cdot\left[\nu\cdot\frac{\partial A_z}{\partial\varphi}\right]=-J_z \quad (8)$$

where A_z, J_z - axial components of vector magnetic potential and vector current density μ specific magnetic resistance (determined by the magnetization curve of the material H (V).

During the calculation of the magnetic field propagation, it is limited to the outer surface of the stator core, where a Dirichlet boundary condition is specified:

$$A_z = 0 \quad (9)$$

A symmetrical three-phase system of phase currents is specified in the stator winding:

$$i_{sA} = I_{ms}\cdot cos(\omega_s\cdot t) \quad (10)$$

$$i_{sB} = I_{ms}\cdot cos\left(\omega_s\cdot t-\frac{2}{3}\cdot\pi\right) \quad (11)$$

$$i_{sC} = I_{ms}\cdot cos\left(\omega_s\cdot t-\frac{4}{3}\cdot\pi\right) \quad (12)$$

where t – time; I_{ms} – the amplitude of the current; $\omega_s = 2\cdot\pi\cdot f_s$ – angular frequency.

At the initial moment when t=0 the currents in phase windings A, B are as follows:

$$i_{sA} = I_{ms} \quad (13)$$

$$i_{sB} = i_{sC} = -0.5 \cdot I_{ms} \qquad (14)$$

A polyphase system of instantaneous current values in the bars of the short-circuited rotor is formed:

$$i_{rj} = \sqrt{2} \cdot I_r \cdot \sin\left(p \cdot \left[(j-1) \cdot \alpha_{rn} + \alpha_{sr} + \alpha_{r1}\right]\right) \qquad (15)$$

where $k = 1,2,...,Q_r$ – number of the slot; $I_{mr} = \sqrt{2} \cdot I_r$ – the amplitude of the phase currents of the rotor; a_{r1} – the coordinate of the first slot (on Figure 1 a_{r1}=0); $a_{rn} = 360° / Q_r$ – the angle of mutual slot displacement.

The magnetic induction, calculated based on the distribution of the magnetic potential using the general expression:

$$\vec{B} = rot\left(\vec{k} \cdot A_z\right) \qquad (16)$$

Its components in polar coordinates

$$B_r = \frac{\partial A_z}{r \partial a}; \; B_a = -\frac{\partial A_z}{\partial r} \qquad (17)$$

From the numerical field calculation, we obtain the electromagnetic torque, which is determined through the Maxwell stress tensor:

$$M_{em} = \frac{l_a}{(r_s - r_r)} \int_{S_\delta} r \cdot f_{T\alpha} dS =$$

$$= \frac{l_a}{\mu_0 \cdot (r_s - r_r)} \int_0^{2\cdot\pi} \int_{r_r}^{r_s} r \cdot B_r \cdot B_\alpha dr d\alpha \qquad (18)$$

where B_r and B_α – the radial and tangential components of the magnetic induction; $\mu_0 = 4 \cdot \pi \cdot 10^{-7}\, H/m$ – magnetic permeability; r_r and r_s – radii of the circles bounding the transverse area of the air gap S_δ from the rotor side and the stator side.

The investigation was conducted using an induction motor with a squirrel-cage rotor of type 4A225M2U3, with a power rating of 55 kW, and a number of pole pairs $p = 1$, the nominal voltage $U = 380/660B$, $\eta = 91\%$; $\cos(\varphi) = 0.92$.

Design parameters:

- the external diameter of the stator $D_a = 0.392$ m;
- the external diameter of the rotor, $D_2 = 0.206$ m;
- the shaft diameter, $D_j = 0.101$ m;
- air gap between the rotor and the stator $\delta = 1$ mm;
- the number of slots in the stator core $Z_1 = 36$;
- the number of slots in the rotor core $Z_2 = 28$.

Figure 7 shows the results of the calculation of the normal component of the magnetic field induction.

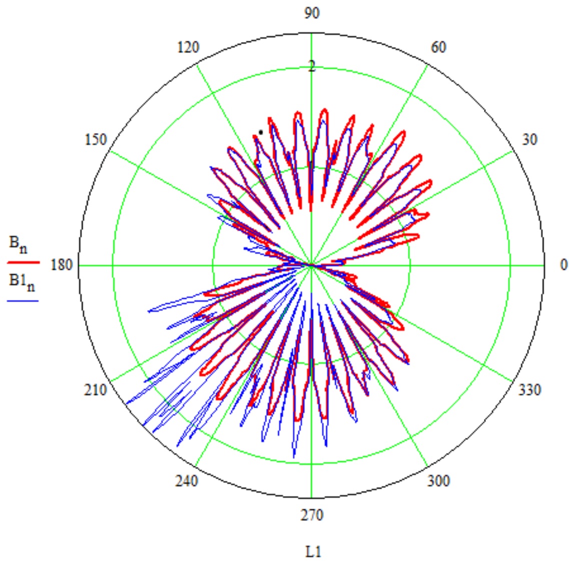

Figure 8. Results of the calculation of the normal component of the magnetic field induction using FEMM software in the polar coordinate system

As seen from Figure 7, under static eccentricity, the amplitude of the magnetic induction at a larger air gap of the motor is significantly lower than that at a smaller air gap, causing unidirectional magnetic pull of the motor; the direction of the magnetic pull aligns with the direction of increasing eccentricity.

Figure 8 shows the results of calculating the time function of the electromagnetic moment within the time interval [0 - T], where T is a time period equal to the time of one complete rotation of the rotor.

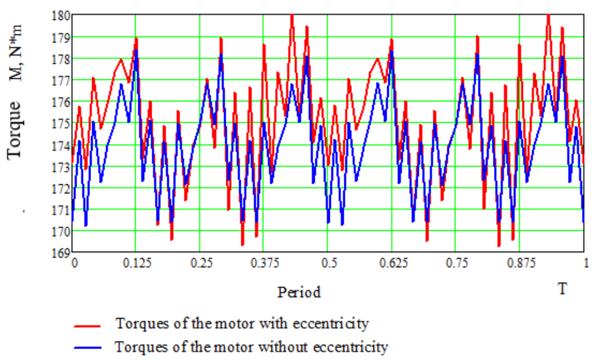

Figure 9. FEMM software calculation results

As seen from Figure 8, with static eccentricity, the amplitude of the electromagnetic torque increases.

A harmonic analysis of the field composition in the air gap of the electric machine has been performed, and the fundamental harmonic of induction as well as higher and lower order harmonics have been identified.

Based on the results of the magnetic field calculation using the post-processor of the program, a text file is generated. This file contains the measured values and the coordinates of the points of the contour where these measurements are taken. The distribution of the normal component of the induction in the air gap is important.

This text file is then read by a program that performs harmonic analysis.

Next, we use the MathCAD program, which has a built-in function FFT (Fast Fourier Transform).

The frequency spectrum of the induction in the air gap with and without eccentricity is presented in Figure 9.

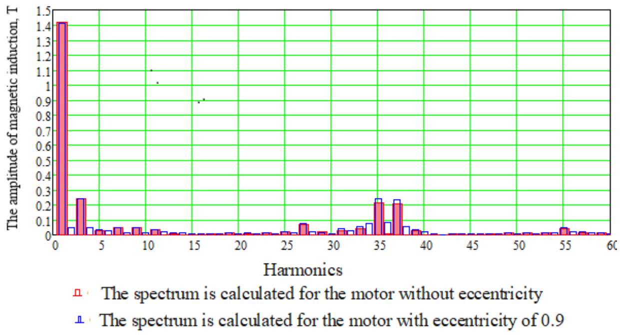

Figure 10. The harmonic composition of the induction in the air gap with the occurrence of eccentricity (blue) and without it (red)

As seen from Figure 10, with static eccentricity, a new order is added to the spectrum.

Therefore, the values of the harmonic orders found using the numerical field method are consistent with those found analytically and with data obtained from open sources [4] – [7], [20], [21].

V. CONCLUSIONS

1. The mathematical model of the two-pole squirrel-cage induction motor has been improved, allowing for more accurate modeling of electromagnetic processes at various values of static rotor eccentricity.

2. The mathematical model implemented in the FEMM package. The simulation results demonstrate that the developed mathematical model of the induction motor enables the detection of a diagnostic relationship between the diagnosed defect (static eccentricity) and the diagnostic feature (higher and lower order induction harmonics in the air gap).

3. In future works, the authors will be provided with the opportunity to improve the obtained mathematical model for modeling rotor eccentricity of an induction motor, taking into account the serration of the stator and rotor.

The timely detection of the presence and magnitude of rotor eccentricity will not only reduce energy consumption costs but also prevent damage to the induction motor.

REFERENCE

[1] Vaskovskiy, Y.N., Geras'kin, A.A. (2014). Vibrational diagnostics of rotor eccentricity in asynchronous machines based on analysis of vibration forces. Bulletin of the National Technical University "KhPI", 38 (1081). 52–62.

[2] Wallin M., Bladh J., Lundin U. (2013). Damper winding influence on unbalanced magnetic pull in salient pole generators with rotor eccentricity. IEEE transactions on magnetics, 49, 9, 5158–5165. URL: https://doi.org/10.1109/tmag.2013.2259633

[3] Novozhilov, A.N. (2013). Diagnostics of rotor eccentricity in alternating current electric machines using artificial neural networks. Bulletin of the National Technical University "KhPI", 1, 68-75.

[4] Geller, B., & Gamata, V. (1981). Higher harmonics in induction machines. M. Energiya, 351.

[5] Novozhilov, A.N., & Isupova, N.A. (2013). Features of modeling the magnetic field in the air gap with rotor eccentricity of an induction motor. Electrical Engineering, 9, 30-33.

[6] Milikh, V.I. (2018). Numerical-field analysis of the adequacy of design data for three-phase asynchronous motors and a method for their refinement based on this. Technical Electrodynamics, 1, 47–55. URL: https://doi.org/10.15407/techned2018.01.047

[7] Yarymbash, D., Kotsur, M., Yarymbash, S., & Kotsur, I. (2017). Osobennosti trehmernogo modelirovanija jelektromagnitnyh polej asinhronnogo dvigatelja [Features of three-dimensional simula-tion of the electromagnetic fields of the asynchronous motors]. Elektrotehnika i elektroenergeti-ka, 2, 43-50. (in Russian) DOI:10.15588/1607-6761-2016-2-5

[8] Chen H., Bi C. (2022). An effective method for determination and characteristic analysis of induc-tion motor parameters. IET electric power applications. 16 (5), 605–615. URL: https://doi.org/10.1049/elp2.12180

[9] Milikh, V.I. (2018). Automated system for forming calculation models of electric machines for the FEMM software environment. Technical Electrodynamics, 4, 74–78. URL: https://doi.org/10.15407/techned2018.04.074

[10] Thomson W. T. (1999). A review of on-line condition monitoring techniques for three-phase squirrel-cage induction motors-past present and future. Keynote address at IEEE symposium on diagnostics for electrical machines, power electronics and drives, 3-18.

[11] Vigovsky, O.V. (2018). Diagnosis of induction motors of nuclear power plant units. Problems of nuclear power plant safety and Chernobyl, 36–40. URL: https://doi.org/10.31717/1813-3584.18.31.4

[12] Lushchik, V.D., Polezin, S.Yu., & Antypko, G.S. (2013). Premature failure of windings in two-pole medium-power induction motors. Electrical Engineering and Electromechanics, 6, 37-39.

[13] Novozhilov, A.N., et al. (2013). Diagnosing rotor eccentricity of an induction motor based on the rootmean-square value of additional harmonic stator currents. Technical Sciences - From Theory to Practice, 27, 1.

[14] Nikiyan, N.G. (2003). Multiphase real asynchronous machine: mathematical modeling, methods, and diagnostic tools: monograph

[15] Petukhov, V.S. (2005). Diagnosis of the state of electric motors based on spectral analysis of consumed current. Electrical Engineering News, 31, 23–26.

[16] Neelam Mehala (2010). Detecting of bearing faults of induction motor using Park's vector approach. *International Journal of Engineering and Technology*, 2. 263–266.

[17] Zhou G.Y., Shen J.X. (2017). Rotor notching for electromagnetic noise reduction of induction motors. IEEE transactions on industry applications, 53(4), 3361–3370.
URL: https://doi.org/10.1109/tia.2017.2681969

[18] J. Du et al. (2021). Research on radial electromagnetic force and vibration response characteristics of squirrel-cage induction motor fed by PWM inverter. IEEE transactions on applied super conductivity, 31, (8). 1–4.
URL: https://doi.org/10.1109/tasc.2021.3096501

[19] Gashimov, M.A., & Mirzoyeva, S.M. (2002). Investigation for the purpose of diagnosing electromagnetic processes in electrical machines with uneven air gap. Electricity, 11, 52-45.

[20] Novozhilov, A.N., & Isupova, N.A. (2012). Investigation of methods for modeling air gap size with rotor eccentricity in an electric machine. *Bulletin of the National Technical University "KhPI"*, 6, 23-28.

[21] Yondem, M.E., Nikiyan, N.G., & Akopyan, G.S. (1985). Magnetic conductivity of the air gap of an induction machine with rotor eccentricity. *Electromechanics*, 5, 32-35.